Optical Coherence Tomography Denoising by Means of a Fourier Butterworth Filter-based Approach

Gabriela Samagaio[1], Joaquim de Moura[1], Jorge Novo[1], and Marcos Ortega[1]
{gabriela.samagaio, joaquim.demoura, jnovo ,mortega}@udc.es

University of A Coruña - Department of Computing, A Coruña (Spain)

Abstract. Optical Coherence Tomography (OCT) is affected by ubiquitous speckle noise that difficult the visualization and analysis of the retinal structures. Any denoising strategy should be able to remove efficiently the noise as well as preserves clinical information contained in the images. This information is crucial to analyses the retinal layer tissue that allows the posterior analysis and recognition of relevant diseases as macular edema or diabetic retinopathy.

To address this issue, a method based on the Fourier Butterworth filter combined with a contrast enhancement and a histogram regularization was developed in order to reduce the speckle noise in OCT retinal images. The proposed method was validated using 45 OCT retinal images organized into 3 groups of noise degree, comparing the results with the performance of representative methods of the state-of-the-art. The validation and comparison were made through three quantitative metrics: Signal-to-Noise Ratio (SNR), Contrast-to-Noise Ratio (CNR) and average Effective Number of Looks (ENL).

The experimental results showed that the proposed method offered satisfactory results, outperforming the results of the other methods by the achievement of a SNR of 7.04 dB and a CNR of 14.08 dB better than the second best filter, respectively, for the whole group of OCT retinal images.

Keywords: Optical Coherence Tomography, retinal imaging, speckle noise, denoising, Fourier Butterworth filter

1 Introduction

Optical Coherence tomography (OCT) is an imaging technique for the analysis of the eye fundus that provides a non-invasive and contactless cross-sectional retinal visualization with high resolution. It has been widely used in biomedical imaging, as in the extraction of medical information as spatial information but also in the measurement of biological tissues such as retinal layers [1–3] and other structures [4, 5], in a micro scale way.

In OCT, speckle noise can be introduced in the capture process by many causes like the eye motion of the patient, multiple scattering or particular properties

of each OCT system [6]. Therefore, the process of denoising of ophthalmic OCT images is essential to obtain better quality images that may lead to a better identification of the retinal structures as well as a better recognition and quantification of different retinal diseases, thus aiding the diagnosis made by the clinicians [7]. For speckle noise reduction, two major strategies are applied at different capture stages: (1) during image acquisition and (2) at a post-processing stage. The first strategy is usually performed by the device at the moment of the image capture, by the use of multiple uncorrelated recordings that are combined to produce the final image. The second stage requires a post-processing of the OCT scans based on computational algorithms [8]. A large variety of post-processing methods have been proposed for speckle noise reduction of OCT slices. In the literature, there are several OCT denoising techniques that are being adapted from other domains as active radar, synthetic aperture radar (SAR) or ultrasound, among others, since the granular noisy pattern is similar to the noise that appear in OCT scans [8]. Therefore, a substantial amount of signal processing research has been conducted to combat speckle noise and, in the last years, new versions of standard denoising filters [9] were adapted to the task of OCT image denoising [10, 11]. Most of them were originally applied to other domains, such as the Lee filter [12], Kuan filter [13] and Frost filter [14], wavelet filter [15], general Bayesian filter [16] or anisotropic diffusion [17], which are the most widely discussed as spatial adaptive filters noise attenuation. Despite the efforts, it is being a challenge to develop an efficient speckle noise reduction algorithm that simultaneously preserves details such as texture and edge information, ensuring that the particular anatomy of those structures are preserved, beyond the image quality metrics, as signal-to-noise-ratio (SNR), contrast-to-noise-ratio (CNR) or average effective number of looks (ENL), that are typically used to measure any denoising strategy.

In this paper, we propose a new method for speckle noise reduction in OCT images based on the application of the Fourier Butterworth filter in combination with an image enhancement and histogram regularization. The method ensures, at the same time, image detail as well as preservation of particular morphological structures, allowing the possible recognition of pathologies in the internal retinal tissue. To validate the method, a comparative analysis with algorithms of the state-of-the-art was developed and implemented for an automatic calculation of quality images metrics, such as SNR, CNR and ENL and using three representative image sets of progressive noise complexity.

2   Methodology

To reduce the speckle noise in OCT retinal images the proposed method is based on the Fourier Butterworth filter. This low pass filter minimizes high frequency components which are essentially the aimed noise. Then, to enhance the image contrast, a post-processing stage based on histogram correction was applied to highlight the morphological structures as retinal layers and pathological structures.

Moreover, in order to develop a systematic comparison between the proposal with methods of the state-of-the-art, an automated iterative regions of interest (ROIs) extraction was implemented, ensuring an independent and objective process on the determination of quantitative metrics such as SNR, CNR and ENL.

2.1   Fourier Butterworth Image Filtering

Fourier Butterworth filter is a low-pass filter where images are transformed from the spatial to the frequency domain and vice-versa. It is characterized as a smooth filter where the high frequencies are cutoff, reducing the noise while preserving, simultaneously, the edges. The filter is governed by two main parameters: the critical frequency and the order filter [18]. The critical frequency determines the transition zone where amplitude of the frequency drops from 1 down to 0, while the order determines its steepness, such that a higher order produces a narrower transition zone [19].

Butterworth filter is applied in OCT images for speckle noise reduction following, as shown in the diagram of blocks in Fig. 1, the next steps: (1) fast Fourier transform (FFT), (2) Transfer Function $H(u,v)$, (3) inverse Fourier transform (IFFT). Based on spatial information of the input noisy image, a meshgrid array is created in order to process the information in frequency domain, which corresponds to the first process block of the diagram.
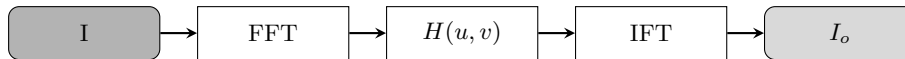

Fig. 1. Basic flow diagram of speckle noise reduction for OCT images based on Fourier Butterworth filter.

There, I is the input noise image and I_o is the output Fourier Butterworth filtered image. The second process block represents the transfer function $H(u,v)$ of the Butterworth low-pass filter of order n at a distance from the origin, defined by:

$$H(u,v) = \frac{1}{1 + (\frac{D(u,v)}{D_0})^2} \tag{1}$$

where, $D(u,v)$ is the distance from point (u,v) to the center of the filter and D_0 is the cutoff frequency. Having calculated $H(u,v)$ a multiply operation is applied with the Fourier transform of an original image, $F(u,v)$, as:

$$G(u,v) = H(u,v) \times F(u,v) \tag{2}$$

Finally, the resultant image, $G(u,v)$ is returned from the frequency to the spacial domain applying IFFT.

2.2 Post Processing

The Fourier Butterworth filter minimizes the presence of noise, Fig. 2 (b). However, it is necessary to enhance the visualization of the morphological structures such as retinal layers that appear in the eye fundus in order to facilitate the posterior analysis. In an attempt to enhance these structures, two main steps were taken: a weighted multiplicative operation of the output Fourier Butterworth filter by the original image and a histogram correction.

Firstly, the resultant image of the Fourier Butterworth filter is multiplied by the original image with a weight $w = 1.2$, empirically calculated in order to enhance the boundaries of retinal layers, as well as preserving the details of the tissue of the morphological structures, as shown in Fig. 2(c).

Then, as a second step, a histogram correction was introduced to regularize the image contrast based on the histogram, as shown in Fig. 2(d), resulting in a more detailed and clear image.
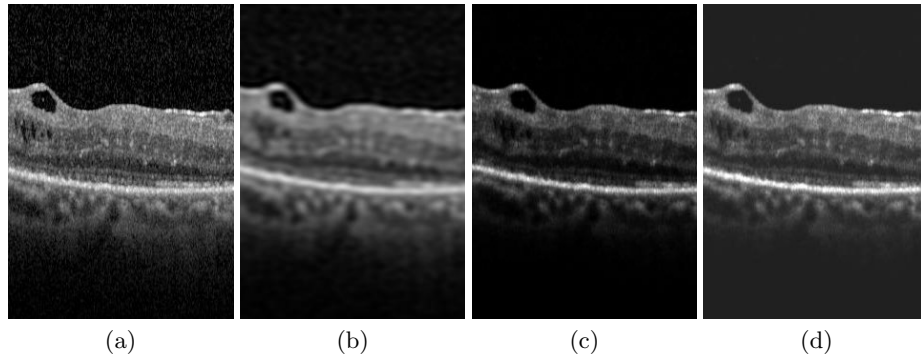

| (a) | (b) | (c) | (d) |

Fig. 2. Example of the post-processing stage of the OCT retinal images. (a) Original noisy image. (b) Output Fourier Butterworth filtered image. (c) Original image correction using the Fourier Butterworth output filter. (d) Contrast enhancement and histogram correction.

2.3 Automatic Validation Process

In order to validate and compare the proposed methodology with reference methods of the literature, quantitative image metrics were calculated, such as SRN, CNR and ENL, as some of the most used metrics in other denoising approaches as classification metrics for speckle noise reduction. However, the presence of pathological structures in the OCT images makes the scenario of image denoise quantification more complicated, since the pathological regions, black non-reflective spaces [20], can alter erroneously this metrics. In order to minimize this limitation, we implemented an automatic method for the extraction of a background and retinal layer ROIs that are needed for the calculation of the implemented

metrics. Two main steps were implemented: an automatic segmentation of the retinal layers and the automatic ROIs extraction.

Automatic segmentation of retinal layers: The calculation of the implemented metrics needs the selection of ROI windows in the background and inside the retinal layer tissue. To automatize this process, we need to identify the limits of these retinal layers. Based on the work of Chiu *et al.* [21], we implemented the identification of the boundaries of retinal tissues in OCT images. This automatic approach for segmenting retinal layers uses graph theory and dynamic programming to represent each OCT image as a graph of nodes, connecting optimum paths from both sides of the image. Firstly, the algorithm calculates dark-to-light gradient images, identifying adjacent layers and generating weights for the layer segmentations. The minimum weighted paths are found by the Dijkstra's algorithm [22] to progressively identify the main layers of the retina. This approach detects eight different layers. However, for this purpose, only the Inner Limiting Membrane (ILM) and the Retinal Pigment Epithelium (RPE) layers were used, as they delimit the retinal layer region.

Automatic ROIs extraction: As second step, an iterative and random process of seed generation and ROI construction was implemented. The seed coordinates are needed to construct m^{th} ROI windows inside the retinal layers as well as 1 background ROI window. Based on these seeds, which are obtained from the original noisy image between the ILM and RPE retinal layers, it is possible to obtain the ROIs in exactly the same coordinates on the returned filtered images to measure the degree of improvement before and after the denoising process. In order to ensure that the quality metrics will not be influenced by pathological structures, 50 random repetitions were executed in an automatic way obtaining as a result the final quality metric means. Moreover, each set of random positions is used with all the methods, certifying that the approaches are all under the same conditions. The positions represent the upper left coordinates of mth ROIs, as shown in Fig. 3, and each ROI will be a window with a size of 10×20 pixels. The background ROI is obtained from the upper left part of the each OCT filtered image, having a total area equal to the sum of the mth ROIs areas, as:

$$A_b = \sum_{m=1}^{m} A_m \tag{3}$$

where, A_b is the background total area and A_m are the area of each mth ROIs.

The quality metrics, SNR, CNR and ENL, provide relevant information about the noise signal, contrast and homogeneity in images, respectively, and are defined as:

$$SNR_m = 20 \cdot log_{10}(\frac{\mu_m}{\sigma_b}) \tag{4}$$

$$CNR_m = \frac{\mu_m - \mu_b}{\sqrt{\sigma_m^2 + \sigma_b^2}} \tag{5}$$

$$ENL_m = \frac{\mu_m^2}{\sigma_m^2} \tag{6}$$

where, μ_b and σ_b are the mean and standard deviation of the background ROI, respectively, while μ_m and σ_m are the mean and standard deviation, of the mth ROIs, respectively. For this purpose, 8 ROIs were selected as m value, for the extraction of the retinal tissue regions, which is a representative and sufficient value to estimate accurately, the quality metrics, having finally:

$$SNR = \frac{1}{8}[\sum_{m=1}^{m=8} SNR_m] \quad CNR = \frac{1}{8}[\sum_{m=1}^{m=8} CNR_m] \quad ENL = \frac{1}{8}[\sum_{m=1}^{m=8} ENL_m] \tag{7}$$
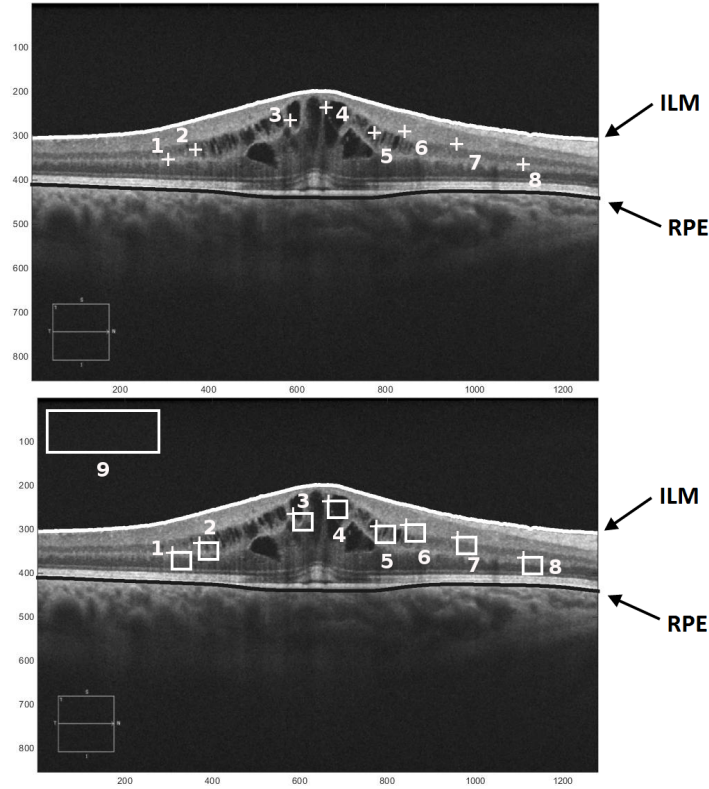

Fig. 3. Example of retinal layers delimitation and ROIs construction. 1st row, iterative random seeds (+) between ILM and RPE layers. 2nd row, ROIs construction where: 1 - 8, retinal layer ROIs; 9, the background ROI.

3   Results and Discussion

We used a dataset composed by 45 OCT retinal images acquired by two different OCT devices: CIRRUS^{TM} HD-OCT Zeiss OCT device and Spectralis® OCT confocal scanning laser ophtalmoscope from Heidelberg Engineering, two of the most representative and used of the market. We used these groups of images with different levels of noise and, therefore quality, each one of them with 15 images: (a) good quality images, (b) mid quality images and (c) bad quality images. Fig. 4 shows representative examples of images included in each group. The vast majority, almost 90% of the images on the dataset belongs to unhealthy retinal patients, increasing the difficulty of the validation process due to the presence of dark regions, typically cystoid regions, that may influence in the metric results.
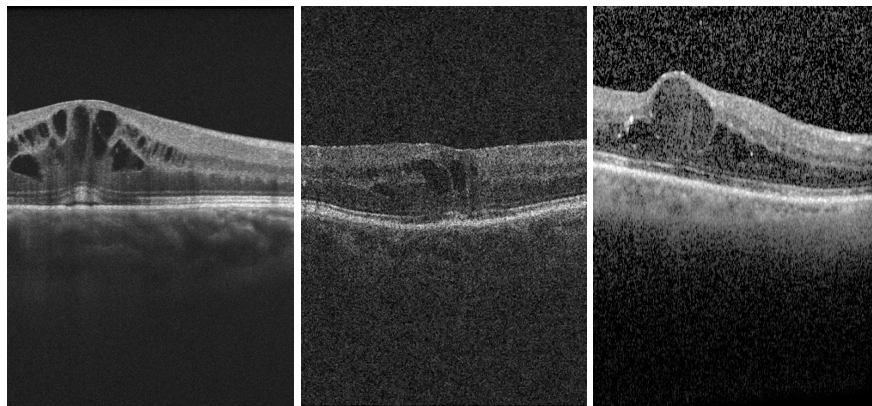

Fig. 4. Example of classification groups of OCT retinal images. (a) Good quality. (b) Mid quality. (c) Bad quality images.

In order to test the performance of the method and perform a fair comparison, we also tested representative denoising methods for OCT images of the state-of-the-art under the same conditions of the proposed methodology. These methods are [10, 11]: Frost filter, Kuan filter, Kuwahara filter, Lee filter and wavelet filter. The proposed method was used with a cutoff frequency equal to $80Hz$ and 5th order, parameters that were empirically established.

The results are synthesized in Fig. 5 which allows to do a quantitative comparison between the original and the filtered images of each quality group. The results show that the proposed method offers a better performance than the rest of the tested methods for all the groups of images in the dataset, having an increase of the SNR parameter from 22.9 dB to 35.6 dB in the group of good quality images and 9.3 dB better than the second best filter, the Frost filter. This demonstrates that the proposed filter suppresses noise in group (a) of images with good quality, but also, similarly positive results were obtained from (b) and (c) groups of images. Further, as expected in group (c) the proposed method

have an improvement of 7.5 dB better than the next best filter, which is Kuan filter and 14.1 dB higher than the original images. Regarding the CNR metric, the proposed method also shows improvements of over 22.1 dB, 6.5 dB and 13.2 dB better than the second best method for (a) to (c), groups of images qualities, respectively. It is also possible to conclude that the image quality classification is coherent with the quantitative metrics, since the best group of original image quality has the highest values for SNR and CNR while the worth group of image quality has the lowest values.

Table 1 presents a general performance analysis and comparison using the entire dataset of 45 images. The three SNR, CNR and ENL were calculated for the original image, the state-of-the-art approaches and the proposed method. The SNR metric of the proposed method increases over 12.74 dB more when compared to the original noisy image and over 7.04 dB than the second best filter, the Kuan filter. Moreover, the proposed method also produced the best image contrast (CNR), near 17.81 dB better than the original image from 4.77 dB to 22.58 dB and 14.08 dB better than the Kuan filter (22.58 dB to 8.50 dB) also the second best method. This reinforces the effectiveness of the proposed method in noise removal conditions with the contrast enhancement of the images and the preservation of the retinal layer tissue details. Regarding the ENL metric, despite the proposal offers a satisfactory score, it is not the best of all of them. However, as this metric measures the homogeneity of the tissue, extremely high values are not desired as they may be derived due to more blurred output filtered images, losing, therefore, retinal tissue details.
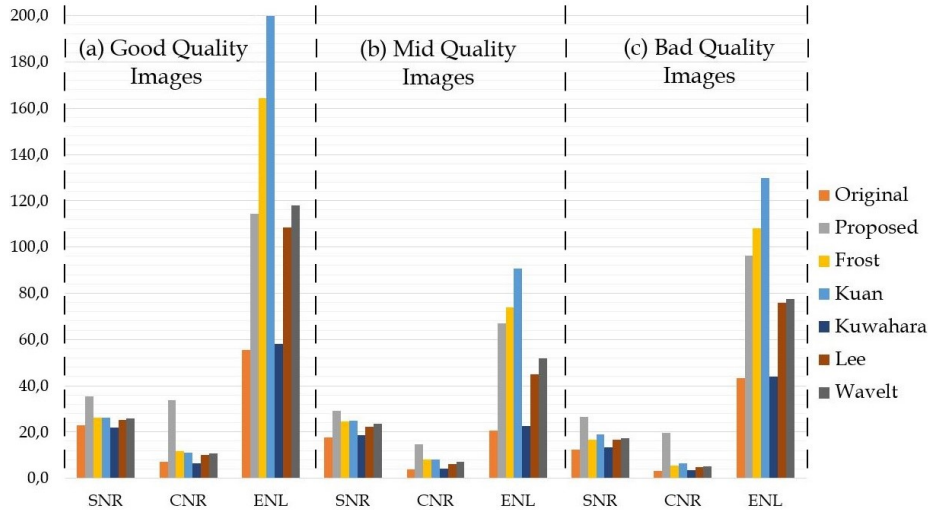

Fig. 5. Results of quality metrics for the tested denoising methods filters on the 3 groups of quality images: (a) Good quality, (b) Mid quality and (c) Bad quality images.

Table 1. Results of the quality metrics SNR, CNR and ENL using the entire dataset.

Method	All Images		
	SNR (dB)	CNR (dB)	ENL
Original	*17.66*	*4.77*	*39.88*
Proposed	**30.41**	**22.58**	92.57
Frost	22.47	8.34	115.42
Kuan	23.36	8.50	**140.07**
Kuwahara	17.97	4.78	41.53
Lee	21.41	7.07	76.44
Wavelet	22.23	7.77	82.42

(a)   (b)   (c)   (d)   (e)   (f)
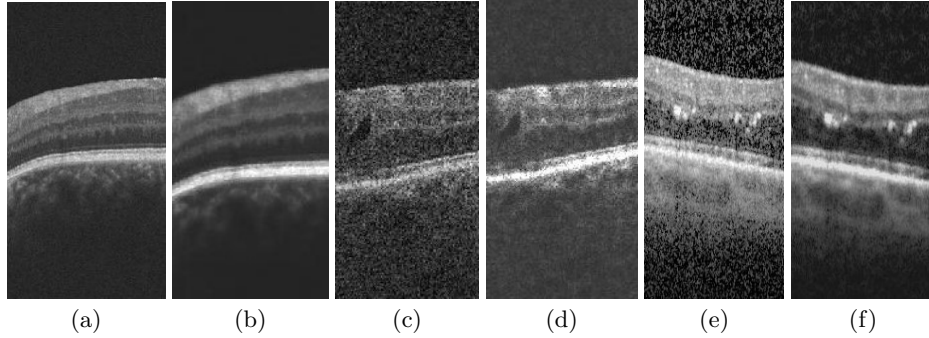
Fig. 6. Example of denoising results in OCT images. (a) Original good quality image. (b) Filtered good quality image. (c) Original mid quality image. (d) Filtered mid quality image. (e) Original bad quality image. (f) Filtered bad quality image.

4   Conclusions

In this paper, we present a new methodology for denoising OCT images based on the Fourier Butterworth filter combined with an image contrast enhancement and histogram regularization. The property of low-pass filter ensures the speckle noise reduction that is present on the OCT images whereas the post-processing with the histogram correction allows an improvement on the image contrast, enhancing the retinal tissue details.

According to the visual assessment of the results before and after filtering the OCT images, it is possible to conclude that the proposed method provides an efficient noise suppression with a higher contrast enhancing of morphological structures such as the boundaries of the different retinal layers, preserving clinical details as cysts without blurring excessively the output image in all the groups of original image qualities. Additionally, based on experimental quality metrics as SNR, CNR and ENL, we can offer an accurate method for noise suppression in comparison with other well-stated methods of the literature. The proposed method returns the best results in SNR, improving over 12.74 dB and 7.04 dB when compared with the original and the second best filtered images, respectively. Moreover, it has a great potential to improve the image contrast (CNR) with 17.81 dB better than original image and 14.08 dB better than the Kuan filter, the second best filter. In this way, the method is capable to improve the conditions of the OCT images, facilitating any posterior analysis of the retinal characteristics in the diagnosis of different retinal diseases.

References

1. D. Huang, E. Swanson, C. Lin, *et al.* Optical Coherence Tomography. *Science (New York, NY)*, 254(5035):1178, 1991.
2. S. Karri, D. Chakraborty, and J. Chatterjee. Transfer Learning Based Classification of Optical Coherence Tomography Images with Diabetic Macular Edema and Dry Age-Related Macular Degeneration. *Biom. Opt. Exp.*, 8(2):579–592, 2017.
3. A. González, M. Penedo, S Vázquez, *et al.* Cost Function Selection for a Graph-Based Segmentation in OCT Retinal Images. In *EUROCAST (2)*, pages 125–132, 2013.
4. J. de Moura, J. Novo, M. Ortega, *et al.* Artery/vein Classification of Blood Vessel Tree in Retinal Imaging. In *Proceedings of the 12th International Joint Conference on Computer Vision, Imaging and Computer Graphics Theory and Applications - Volume 4: VISAPP, (VISIGRAPP 2017)*, pages 371–377, 2017.
5. J. de Moura, J. Novo, M. Ortega, *et al.* 3D Retinal Vessel Tree Segmentation and Reconstruction with OCT Images. In *International Conference Image Analysis and Recognition*, pages 716–726. Springer, 2016.
6. M. Hee, J. Izatt, E. Swanson, and et al. Optical Coherence Tomography of the Human Retina. *Archives of Ophthalmology*, 113(3):325–332, 1995.
7. V. Guedes, J. Schuman, E. Hertzmark, and et al. Optical Coherence Tomography Measurement of Macular and Nerve Fiber Layer Thickness in Normal and Glaucomatous Human Eyes. *Ophthalmology*, 110(1):177–189, 2003.
8. A. Baghaie, R. D'Souza, and Z. Yu. Application of Independent Component Analysis Techniques in Speckle Noise Reduction of Retinal OCT Images. *Opt. Int. J.for Light and Elec. Opt.*, 127(15):5783–5791, 2016.

9. S. Paes, S. Ryu, J. Na, and et al. Advantages of Adaptive Speckle Filtering Prior to Application of Iterative Deconvolution Methods for OCT Imaging. *Optical and Quantum Electronics*, 37(13):1225–1238, 2005.
10. A. Ozcan, A. Bilenca, A. Desjardins, and et al. Speckle Reduction in OCT Images Using Digital Filtering. *J. of the Opt. Soc. of America A*, 24(7):1901–1910, 2007.
11. Harry Salinas and Delia Fernández. Comparison of PDE-Based Nonlinear Diffusion Approaches for Image Enhancement and Denoising in OCT. *IEEE Transactions on Medical Imaging*, 26(6):761–771, 2007.
12. Jong-Sen Lee. Speckle Analysis and Smoothing of Synthetic Aperture Radar Images. *Computer Graphics and Image Processing*, 17(1):24–32, 1981.
13. D. Kuan, A. Sawchuk, T. Strand, and et al. Adaptive Noise Smoothing Filter for Images with Signal-Dependent Noise. *IEEE Trans. on Pattern Anal. and Mach. Int.*, (2):165–177, 1985.
14. V. Frost, J. Stiles, K. Shanmugan, and et al. A Model for Radar Images and its Application to Adaptive Digital Filtering of Multiplicative Noise. *IEEE Trans. on Pattern Anal. and Mach. Int.*, (2):157–166, 1982.
15. M Mayer, A. Borsdorf, M. Wagner, and et al. Wavelet Denoising of Multiframe Optical Coherence Tomography Data. *Biom. Opt. Exp.*, 3(3).
16. A. Wong, A. Mishra, K. Bizheva, and et al. General Bayesian Estimation for Speckle Noise Reduction in OCT Retinal Imagery. *Op. Exp.*, 18(8):8338–8352, 2010.
17. P. Puvanathasan and K. Bizheva. Interval Type-II Fuzzy Anisotropic Diffusion Algorithm for Speckle Noise Reduction in OCT Images. *Optics Express*, 17(2):733–746, 2009.
18. M. Lyra, A. Ploussi, M. Rouchota, and et al. Filters in 2D and 3D Cardiac SPECT Image Processing. *Cardiology Research and Practice*, 2014, 2014.
19. Jennifer Prekeges *et al.* *Nuclear Medicine Instrumentation*. Jones & Bartlett Publishers, 2012.
20. Y. Helmy and H. Atta. Optical Coherence Tomography Classification of Diabetic Cystoid Macular Edema. *Clin Ophthalmol*, 7:1731–7, 2013.
21. S. Chiu, X. Li, P. Nicholas, and et al. Automatic Segmentation of Seven Retinal Layers in SDOCT Images Congruent with Expert Manual Segmentation. *Optics Express*, 18(18):19413–19428, 2010.
22. Edsger W Dijkstra. A Note on Two Problems in Connexion with Graphs. *Numerische Mathematik*, 1(1):269–271, 1959.